XVII IMEKO World Congress
Metrology in the 3rd Millennium
June 22–27, 2003, Dubrovnik, Croatia

INFLUENCE OF THE INDENTER GEOMETRY AND THE MODE CONTROL IN HARDNESS MEASUREMENT BY INSTRUMENTED INDENTATION TEST

Renato R. Machado[1], Tácito B. Pinto[2] and Itamar Ferreira[3]

[1]INMETRO, Duque de Caxias/Xerém, Brasil, [2]CETEC, Belo Horizonte, Brasil and [3]UNICAMP, Campinas, Brasil

Abstract – Taking into account the technical procedures established on ISO/FDIS 14577-1 standard draft [1], instrumented indentation tests (IIT) were carried out on macro range, in order to determine hardness and other material parameters, so that, using a universal testing machine adapted with a system developed for this end [2]. Two different indenters and two different modes of control were used. It was observed that despite using different modes of control the values of the parameters analysed were similar considering the same indenter geometry. Concerning to the different indenter geometries the bigger hardness values was observed for *HV* indenter than *HBW* indenter. Relating to the mechanical work, the results showed in one hand a similar elastic deformation work for both indenters on the other hand it showed a major plastic deformation work for *HV* indenter than the *HBW* indenter.

Keywords: Instrumented Indentation Testing

1. INTRODUCTION

In a near future, the technique of instrumented indentation test (IIT) will be a powerful document for the mechanical properties users, because it will allow the determination of a variety of parameters, quickly and with great versatility, comparing with traditional hardness and tension tests.

In order to analyse the attendance and the contributions of the new metallic materials test for hardness and other parameters in macro range (2 N <F < 30 000 N), it was developed a system taking in advance a universal testing machine and its software to do *IIT*, in spite of the system resolution [3]. The system was performed following the procedure of ISO/FDIS 14577-1 [1] standard draft. Force (F) as well as displacement/indentation depth (h) controls were used in this test, besides the *HV* (Pyramidal) and *HBW* (Spherical) indenters.

The objective of this work was to evaluate the use of different geometries of indenters to determine hardness and other material parameters using different modes of control, i.e., test force and displacement control. The regions of the curves in regards to the plastic deformation and the elastic recovery were considered in this study.

2. METHOD AND PROCEDURE

The instrumented indentation testing method turns on the continuous monitoring of the force and the indentation depth during the whole dwell time, providing not only application but also removal force curves. Residual indentation measurements are not required in this method, so that it eliminates the operator influence. The main parameter given through this test was the Martens Hardness (HM) results, that is obtained by the calculation of the test force (F) and the superficial area of contact ($A_s(h)$), considering the indentation depth (h) and the indenter geometry (in this case a pyramidal square base and a 2,5 mm spherical indenters), see (1), (2) and (3), where *D* is the nominal diameter of Brinell sphere. In this work, the *HM* and H_{IT} values were calculated for maximum test force (F_{max}).

$$HM = \frac{F}{A_s(h)} \tag{1}$$

where $A_s(h)$ for pyramidal indenter is

$$A_s(h) = 26{,}43 \times h^2 \tag{2}$$

and for spherical indenter is

$$A_s(h) = \pi \times D \times h \tag{3}$$

Besides the determination of *HM*, other material parameters, like indentation hardness (H_{IT}) were determined, see (4), (5), (6) and (7).

$$H_{IT} = \frac{F_{\max}}{A_p} \tag{4}$$

where A_p is the projected contact area. For *HV* indenter (5) should be used and for *HBW* indenter (6) should be used.

$$A_p = 24{,}50 \times h_c^{\,2} \tag{5}$$

$$A_p = \pi \times h_c \times (D - h_c) \tag{6}$$

where h_c is the depth of contact between the indenter and the test piece, see (7).

$$h_c = h_{\max} - \varepsilon \times (h_{\max} - h_r) \quad (7)$$

where h_{max} is the maximum indentation depth, h_r is the point of intersection of the tangent to the removal curve at F_{max} with the indentation depth axis. ε is established in [1] and represent the correction factor for different indenter geometries.

The indentation modulus (E_{IT}) was also determined following (8) and (9).

$$E_{IT} = \frac{1-(\nu_s)^2}{\frac{1}{E_r} - \frac{1-(\nu_i)^2}{E_i}} \quad (8)$$

where ν_s is the Poisson's ratio of the test piece, ν_i is the Poisson's ratio of the indenter, E_i is the modulus of the indenter and E_r is the reduced modulus of the indentation contact as shown in (9).

$$E_r = \frac{\sqrt{\pi}}{2C\sqrt{A_p}} \quad (9)$$

With the objective to determine the compliance of the contact (C) (*dh/dF* at F_{max}), the test force removal curve using a polynomial of second order was fitted.

The plastic and elastic deformation of the indentation work (η_{IT}, W_{plast}, W_{elast}) were calculated in accordance to [1]. They are represented by the parts of the areas under the curves during the indentation and removal of the test force.

The system used in this work, was a universal testing machine operating in compression mode, carring out a force transducer of 9806,65 N (1000 kgf) with 100 % of full scale. To monitor the test displacement a Linear Variable Differential Transducer (LVDT) was used with 10 mm of stroke.

In this work, a Brinell standard reference block (261 HBW2,5/187,5), a pyramidal indenter of diamond square base (HV) and a hard metal spherical indenter (HBW) with 2,5 mm of diameter, were used to carry out measurements of *IIT*, all of them with calibration certificate. The nominal test force used for all testing was 1839 N (187,5 kgf).

The rate used for tests with force control was 98 N/s (10 kgf/s) during the application and removal of the test force. The whole cycle was around 37 s, without any time (t) of maintenance of F_{max} = 1839 N (187,5 kgf) for both indenters, see Figs. 1 and 2. The rate used for the test with displacement control was 0,01 mm/s during the application and the removal of the test force, also without any time of maintenance of F_{max}. The full cycle was around 26 s for *HV* indenter and 20 s for *HBW* indenter, see Figs. 1 and 2.

3. RESULTS AND DISCUSSIONS

In this work, different studies were done in order to obtain different material parameters in the macro range, like hardness (HM and H_{IT}), modulus (E_{IT}) and mechanical work (W_{total}, W_{plast} and W_{elast}). All of them were calculated considering two types of indenter (HV and HBW) and two types of control (force and displacement).

The use of different modes of control provided some characteristics concerning to the cycle test force as presented in Figs. 1 and 2 for *HV* indenter and *HBW* indenter respectively. Taking into account that the rates of the test force and the displacement were constant during the whole test cycle, it can be seen that, independently from the indenter geometry used, the test force cycle was symmetric during the application and removal of the test force in the force control and asymmetric in the displacement control. It can also be observed in Fig. 1 that the use of the force rate of 98 N/s and the displacement rate of 0,01 mm/s provided a similar time of the test force application (≈19 s) for *HV* indenter. For *HBW* indenter, see Fig. 2, the use of the same rates presented different time of the test force application (≈13 s for displacement control and ≈19 s for test force control). This can be related to the different indenter geometries resulting in different deformations into the standard block.

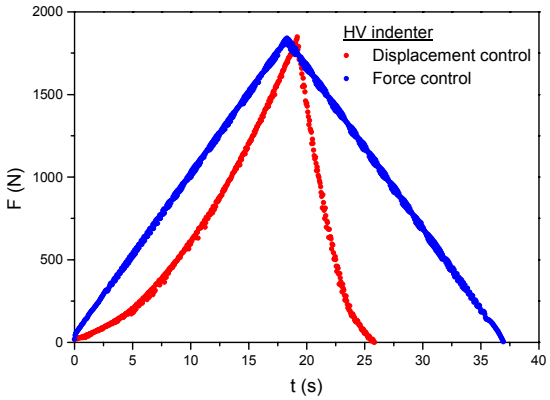

Fig. 1. *F* versus *t* with *HV* indenter.

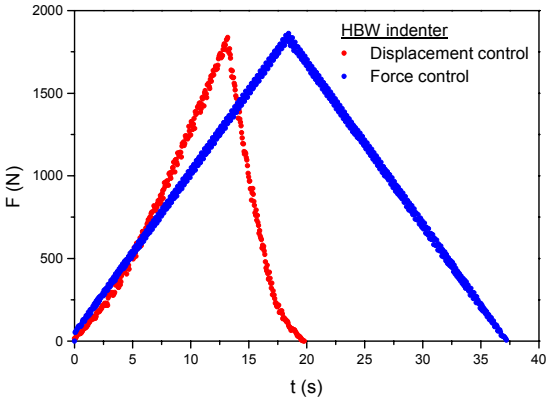

Fig. 2. *F* versus *t* with *HBW* indenter.

Fig. 3 shows the curves obtained by *IIT* with displacement control, using as *HV* as *HBW* indenters. It can be seen that the slope of the curves during the force removal (elastic recovery), was similar. Moreover, the slope curves of the displacement control, showed that the test with *HV*

indenter got higher indentation depth than the *HBW* indenter for the same F_{max} used. This can be related to the different stress fields generated by the different indenter geometries, for the same maximum test force.

Fig. 4 shows the curves of force (F) versus time (t) and indentation depth (h) versus time (t) related to *F x h* curves of Fig. 3. Analysing the *F x t* curve with *HBW* indenter the major homogeneity between increase and decrease of the curves can be seen in comparison to the *F x t* curve with *HV* indenter. Fig. 4 shows also a lower dwell time in regards to *HBW* indenter, for the same F_{max} and displacement rate used.

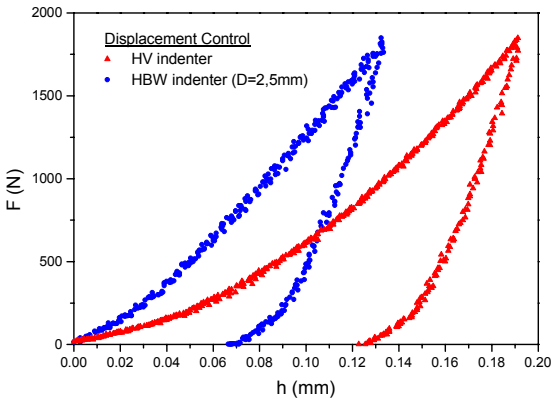

Fig. 3. *F* versus *h* with displacement control.

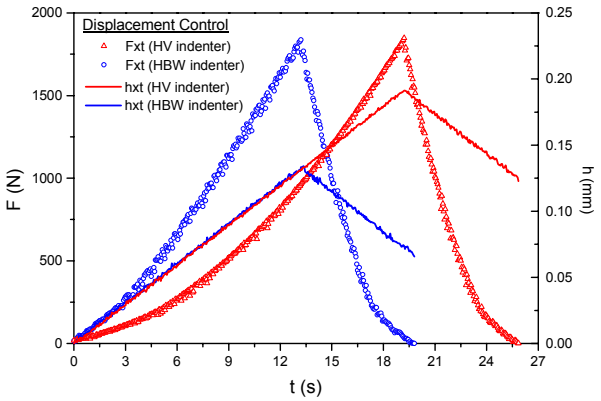

Fig. 4. *F* and *h* versus *t* with displacement control.

The *h x t* curve in Fig. 4 shows that the test made with displacement control provided the same curve of indentation depth for both indenters. Nevertheless, for *HBW* indenter the maximum test force was obtained before *HV* indenter, i. g., with lower test time and indentation depth.

3.1. Hardness

The hardnesses analysed in this work were the Martens and the Indentation hardness using 1839 N of test force. The exception was the item 3.1.3 where the hardness analysis were carried out considering the full test force application cycle.

3.1.1. Martens Hardness (HM)

Table I shows the results obtained by *IIT* for *HM* values and its standard deviation (SD) for 10 measurements into the 261 HBW 2,5/187,5 standard block with test force and displacement control, using *HV* as well as *HBW* indenters. It can be observed that the *HM* values presented some differences, considering the same indenter geometry for both modes of control. This fact can be related to the zero-point definition [3] and the force and displacement rates used.

TABLE I. Results of *HM* and the corresponding *h* and $A_s(h)$ for *HV* and *HBW* indenters by force and displacement control into 261 HBW 2,5/187,5 standard block.

Indenter	h (mm)	A_s(h) (mm^2)	HM (N/mm^2)	SD of HM (N/mm^2)
	Force control			
HV	0,1948	1,0037	1842	131
HBW	0,1450	1,1384	1633	106
	Displacement control			
HV	0,1909	0,9633	1912	141
HBW	0,1330	1,0439	1769	36

It can be observed that the *HM* value obtained for *HBW* indenter was lower than for *HV* indenter for both modes of control. Taking into account the use of the same maximum test force, the lower *HM* value for *HBW* indenter can be related to the major superficial area of contact, in spite of the lower indentation depth, see Table I. This can be seen in Fig. 5 where the *HBW* indenter shows bigger $A_s(h)$ than *HV* indenter for the same indentation depth, up to $h \approx 0{,}3$ mm. Above this value this tendency changes.

As a whole it is supposed that for the same test force and indentation depth up to ≈ 0,3 mm, the *HM* value calculated with *HV* indenter will be bigger than the *HM* value calculated with *HBW* indenter, due to the lower superficial area of contact. Above the value $h \approx 0{,}3$ mm, the *HM* will be lower for the test with *HV* indenter. However, this will depend on the test force applied and the material properties of the test piece, resulting in different *h* and $A_s(h)$.

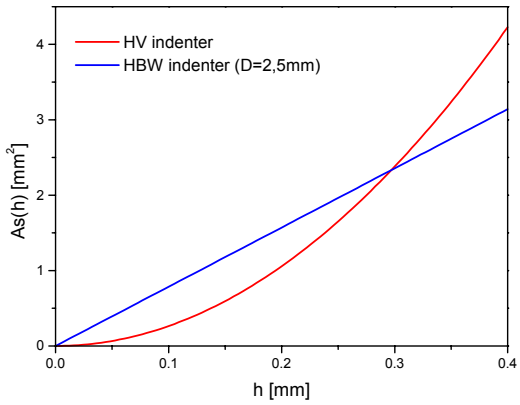

Fig. 5. $A_s(h)$ versus *h*.

3.1.2. Indentation Hardness (H_{IT})

The results of H_{IT} (Table 2) follows the same behaviour of *HM* results. Nevertheless, the differences between H_{IT}, A_p and h_c values using the same mode of control for both indenters were proportionally bigger than *HM*, $A_s(h)$ and *h*. The same observations made for *HM* can be made for H_{IT}.

TABLE II. Results of H_{IT} and the corresponding h_c and A_p for *HV* and *HBW* indenters by force and displacement control into 261 HBW 2,5/187,5 standard block.

Indenter	h_c (mm)	A_p (mm^2)	H_{IT} (N/mm^2)	SD of H_{IT} (N/mm^2)
	Force control			
HV	0,1664	0,6791	2726	213
HBW	0,1174	0,8788	2297	71
	Displacement control			
HV	0,1628	0,6497	2837	163
HBW	0,1046	0,7870	2348	49

Fig. 6 shows that the behaviour of the A_p *x* h_c curves was similar to the $A_s(h)$ *x h* (Fig. 5). It is also verified that the intersection of the curves occurs in a similar indentation depth (h ≈ 0,3 mm).

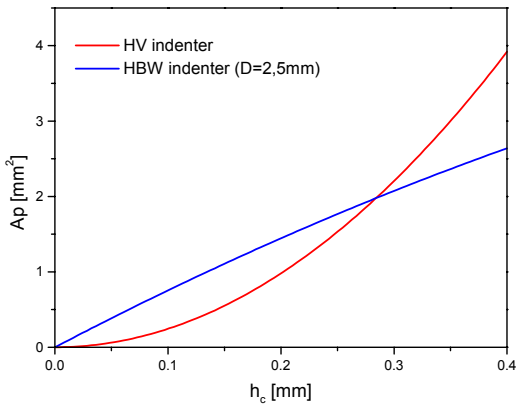

Fig. 6. A_p versus h_c.

3.1.3. Area Function

Fig. 7 shows the curves of Martens hardness versus superficial area, that is a *h* function, carried out by *HV* and *HBW* indenters with displacement control. Fig. 8 shows the curves *F* versus *h* and $A_s(h)$ versus *h* for the same conditions of Fig. 7.

It can be noted in Fig. 8 that the test forces (F) increases in relation to the indentation depth (h) for the same reason that the superficial area of contact (A_s(h)) increases. This implies in an *HM* value more stable in relation to *h* and $A_s(h)$, as observed in Fig. 7, despite the decrease in the *HM* value in the beginning of the indentation depth.

It is also possible to verify in Fig. 8, for the *HBW* indenter, that the test force had a lower increasing in the beginning in function to *h* than $A_s(h)$, giving lower *HM* values for small indentation depths. Using this indenter geometry *h* had a linear relation with $A_s(h)$. Increasing the indentation depth, *F* increased more than $A_s(h)$, thus increasing the *HM* values in relation to *h* or $A_s(h)$, as shown in Fig. 7.

It can be visualised in Fig. 7 the dependence of the Martens hardness in relation to $A_s(h)$, that is linked to the indentation depth and the test force.

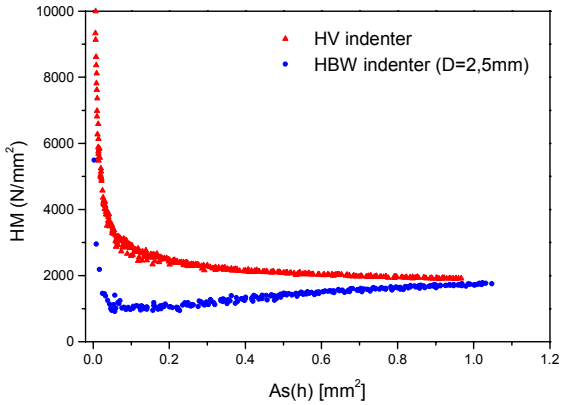

Fig. 7. *HM* versus $A_s(h)$.

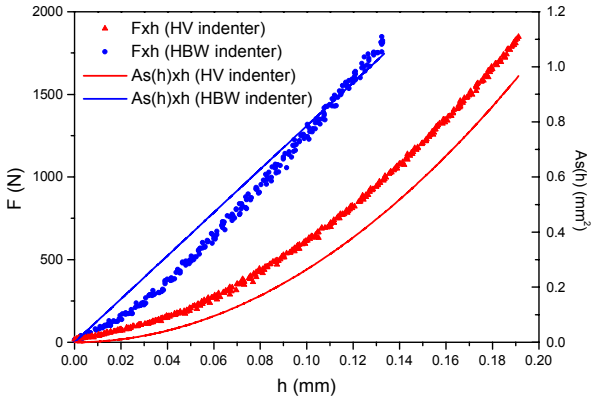

Fig. 8. *F* and $A_s(h)$ versus *h*.

3.2. Indentation Modulus (E_{IT})

Table III shows the indentation modulus results obtained for two modes of control and two indenters into a 261 HBW 2,5/187,5 standard block.

TABLE III. Results of E_{IT} with *HV* and *HBW* indenters by force and displacement control into 261 HBW 2,5/187,5 standard block.

Mode controlled	E_{IT} (N/mm^2)			
	Mean value	SD	Mean value	SD
	HV indenter		HBW indenter	
Force	56352	2577	53034	1953
Displacement	56291	2743	54087	1412

It can be observed by the Table III analysis the agreement between the values of the indentation modulus despite the mode of control and the indenter geometry used. Those facts suggest the same elastic behaviour independently of the indenter geometry.

3.3. Indentation work

Tables IV and V shows the results of the mechanical work analysed, i.g., the elastic deformation work of indentation (W_{elast}), the plastic deformation work of indentation (W_{plast}), the total mechanical work of indentation (W_{total}) and the elastic part of indentation work (η_{IT}).

TABLE IV. Results of mechanical work with *HV* and *HBW* indenters by force control

Force control				
Parameters	HV indenter		HBW indenter	
	Mean	SD	Mean	SD
W_{elast} (N.m)	0,0423	0,0019	0,0411	0,0023
W_{plast} (N.m)	0,0909	0,0007	0,0675	0,0006
W_{total} (N.m)	0,1332	0,0021	0,1085	0,0024
η_{IT} (%)	31,8		37,9	

TABLE V. Results of mechanical work with *HV* and *HBW* indenters by displacement control.

Displacement control				
Parameters	HV indenter		HBW indenter	
	Mean	SD	Mean	SD
W_{elast} (N.m)	0,0410	0,0017	0,0416	0,0019
W_{plast} (N.m)	0,0887	0,0011	0,0645	0,0006
W_{total} (N.m)	0,1297	0,0015	0,1061	0,0022
η_{IT} (%)	31,6		39,2	

It is possible to observe, in both tables, the similarity between the values of W_{elast} related to the modes of control and the indenter geometries. Thus as the indentation modulus (E_{IT}) the elastic work (W_{elast}) showed to be an intrinsic material property regardless the different test conditions used. With relation to the W_{plast} the results showed major values for *HV* indenter than *HBW* indenter, approximately 36 %. This can be related to the different stress fields generated by the different indenter geometries.

The total work presents major values for *HV* indenter due to the major plastic work. The relation η_{IT} was similar concerning to the modes of control and lower for the *HV* indenter comparing to *HBW* indenter because of the major W_{total} and similar W_{elast}.

4. CONCLUSION

Taking into account the limitations of the systems used it was possible to conclude that the results obtained showed a few influence of the mode control for the studied parameters. It was also observed a major dispersion in force control comparing with displacement control, maybe due to the definition of zero-point by the used system. The difference between the values of the parameters measured for the different modes of control and the same indenter geometry can be related to the different rates used.

Differences were verified by the use of different indenter geometries in regards to the hardness values, maybe caused by different stress fields on the test piece.

Analysing the results of the indentation modulus and the mechanical work, it is possible to perceive the intrinsic elastic properties of the material, given a similar elastic recovery for the test carried out.

The results of the test taken with *HV* indenter presented major values for the plastic deformation work of indentation.

It was verified major hardness values by the use of the *HV* indenter, considering the maximum test force and the consequent indentation depth achieved, which were lower than the intersections of $A_s(h) \, x \, h$ and $A_p \, x \, h_c$ for both indenters.

REFERENCES

[1] ISO/FDIS 14577-1 Metallic materials – Instrumented indentation test for hardness and materials parameters – Part 1: Test method.

[2] T. B. Pinto *"Mechanical behaviour of a type 2205 duplex stainless steel as a function of the temperature and of the brittle phase precipitation"* "Comportamento mecânico de aço inoxidável duplex, sob a influência da temperatura e da precipitação de fases frágeis". *Doctorate thesis, FEM/UNICAMP,Campinas, Brazil, 2001.*

[3] R. R. Machado, T. B. Pinto and I. Ferreira. "Comparison Between Conventional Rockwell Hardness Testing and Instrumented Indentation Testing". To be published in the XVII IMEKO World Congress, Metrology in the 3rd Millennium, June 22–27, 2003, Dubrovnik, Croatia.

Authors: Mechanical Engineer, M.Sc., Renato R Machado (Force, Torque and Hardness Laboratory/National Institute of Metrology, Standardization and Industrial Quality – Inmetro), Av. N. S das Graças, 50, Xerém, CEP: 25250-020, Duque de Caxias/RJ, Brasil, phone: (+55 21) 21 2679-9068, fax: (+55 21) 21 2679-1505, e-mail: rrmachado@inmetro.gov.br. Mechanical Engineer, D.Sc., Tácito B. Pinto (Setor de Desenvolvimento Tecnológico/Fundação Centro Tecnológico de Minas Gerais – CETEC), Av. José Cândido da Silveira, 2000, Horto, CEP: 31170-000, Belo Horizonte/MG, Brasil, phone: (+55 21) 31 3489-2355, fax: (+55 21) 31 3489-2200, e-mail: tacito@cetec.br. Mechanical Engineer, D.Sc., Itamar Ferreira (Departamento de Engenharia de Materiais - FEM/UNICAMP), C.P. 6122, CEP: 13083-970, Campinas/SP, Brasil, phone: (+55 21) 19 3788-3312, fax: (+55 21) 19 3788-2389, e-mail: itamar@fem.unicamp.br.